Partially Homogenous Charge Compression Ignition Engine Development for Low Volatility Fuels

2 authors:

Akhilendra Pratap Singh
Indian Institute of Technology Kanpur
102 PUBLICATIONS   **3,619** CITATIONS

Avinash Kumar Agarwal
Indian Institute of Technology Kanpur
582 PUBLICATIONS   **23,244** CITATIONS

Partially Homogenous Charge Compression Ignition Engine Development for Low Volatility Fuels

Akhilendra Pratap Singh and Avinash Kumar Agarwal*

Engine Research Laboratory, Department of Mechanical Engineering, Indian Institute of Technology Kanpur, Kanpur 208016, India

ABSTRACT: Control of harmful pollutants such as oxides of nitrogen (NOx), particulate matter (PM)/ soot, carbon monoxide (CO), and hydrocarbons (HC) emitted by diesel engines is essential in order to protect the environment and human health. Different versions of low temperature combustion (LTC) concepts have shown their potential in controlling these pollutants, while achieving thermal efficiencies similar to conventional compression ignition (CI) engines. In this study, a diesel fueled partially premixed homogeneous charge compression ignition (PHCCI) engine was investigated to explore the feasibility of LTC combustion. All experiments were performed on a constant speed two cylinder engine prototype, in which one cylinder was modified to operate in PHCCI combustion mode and the other cylinder operated in conventional CI combustion mode. An external mixing device, called a "fuel vaporizer", was developed for partially homogeneous fuel-air mixing. For a better understanding of the effect of intake charge temperature (T_i) and exhaust gas recirculation (EGR), experiments were performed at three different T_i's (160, 180, and 200 °C) and three different EGR rates (0, 10, and 20%) at six engine loads with a relative fuel-air ratio (λ) ranging from 1.5 (rich limit) to 5.25 (lean limit). Experimental results showed that fuel-air mixing was significantly affected by T_i. At higher engine loads, higher heat release rate (HRR) of PHCCI combustion led to excessive knocking. Combustion phasing was found to be the most important parameter in PHCCI combustion, which affected combustion, performance, and emission characteristics. Increasing T_i improved fuel-air mixing, leading to superior combustion as well as lower HC and CO emissions. However, at 200 °C, excessive knocking deteriorated PHCCI engine performance and led to higher NOx emissions. Increasing the EGR rate effectively controlled PHCCI combustion, leading to lower HRR and NOx emissions. However, too high EGR rate increased the CO, HC, and PM emissions, primarily due to relatively lower combustion chamber temperatures. This study showed that selection of suitable control parameters (such as T_i and EGR rate) led to superior PHCCI combustion, which could possibly extend the operating load range and engine operating window and may be useful in developing a practical and efficient LTC engine.

1. INTRODUCTION

Compression ignition (CI) and spark ignition (SI) engines are mainly reliable and established power plants for the automotive sector. Over the past several decades, diesel engines have become more efficient, durable, quieter, and vibration-free. Different active and passive emission reduction techniques have been developed to meet prevailing emission norms. These methods/techniques mainly include in-cylinder combustion optimization and exhaust gas after-treatment, which have been developed over decades. Three-way catalytic convertor (TWC), diesel oxidation catalyst (DOC), diesel particulate filter (DPF), selective catalytic reduction (SCR), and lean NOx trap (LNT) are popular exhaust gas after-treatment techniques. However, the cost and complexities involved limit the application of these after-treatment devices in diesel engines. The trade-off between oxides of nitrogen (NOx) and particulate matter (PM) emitted by diesel engines is another concern, which remains a main area of improvement.[1−3] NOx emissions from diesel engines react with atmospheric moisture, leading to acid rain.[2]

A low temperature combustion (LTC) concept has evolved over the last two decades in response to demand for simultaneous NOx and PM emission reduction from direct injection (DI) diesel engines. LTC is capable of delivering higher thermal efficiencies from gasoline engines and ultralow NOx and PM emissions from diesel engines, which makes it a very strong potential alternative technology to the existing technologies. Initially Onishi et al.[4] implemented homogeneous

charge compression ignition (HCCI) in a two-stroke gasoline engine. Najt and Foster[5] investigated HCCI combustion in a 4-stroke engine and called it 'compression ignition homogeneous charge' (CIHC) combustion. They reiterated that there was no flame front in CIHC engines. Thring[6] introduced HCCI combustion and investigated the effects of external exhaust gas recirculation (EGR) and air−fuel ratio on this combustion mode. Since the 1990s, the HCCI concept has become an attractive research topic worldwide, and different methodologies have been developed to attain gasoline HCCI combustion.[7,8]

After validation of advantages of HCCI combustion in gasoline engines, researchers focused on attaining mineral diesel fueled HCCI combustion. Charge preparation, i.e. fuel-air mixing, was the most important requirement in HCCI combustion. For mineral diesel fueled HCCI combustion, extremely low volatility of mineral diesel was the main challenge, which affected homogeneous charge formation. Initially, in-cylinder mixture preparation using early direct injection[9−13] and late direct injection[14,15] was employed in mineral diesel fueled HCCI engines; however, lack of fuel-air

mixture homogeneity from these techniques resulted in inferior combustion.

For mineral diesel, port fuel injection (PFI) was found to be the easiest way to obtain a partially homogeneous fuel-air mixture. This is an external mixture preparation technique, based on diesel fumigation at higher temperatures.[16] With this technique, turbulent flow velocities at the intake port promoted fuel-air mixing, leading to formation of more homogeneous charge. Gray et al.[17] achieved mineral diesel fueled HCCI combustion using intake air preheating and EGR as main control parameters. These control parameters were varied depending on engine load and the compression ratio used. Combustion phasing retarded with increasing EGR, which resulted in relatively higher hydrocarbon (HC) and carbon monoxide (CO) formation due to relatively lower in-cylinder temperatures. At lower intake temperature (T_i), the PFI mixture formation technique led to lower fuel evaporation and inhomogeneous fuel-air mixture formation as well as increased fuel impingement on the cylinder walls, leading to higher HC and CO emissions, higher fuel consumption, and lubricating oil dilution.[17−20] A higher boiling range of mineral diesel resulted in poor evaporation of the fuel, and non-evaporated fuel adhered to the intake manifold and combustion chamber walls. To resolve this issue, higher inlet air temperatures were used to vaporize mineral diesel. This resulted in advanced combustion phasing, which reduced HC and CO emissions. Raising the intake air temperature reduced fuel wall-film formed in the intake manifold, which subsequently reduced HC emissions; however, they still remained on the higher side.[21] However, significant cool combustion chemistry of mineral diesel limited the use of this technique.[18] During the compression stroke, when the temperature of the mineral diesel-air mixture exceeded 800 K, rapid autoignition in the combustion chamber led to excessive knocking. The increased intake air temperature also reduced the power density of HCCI engines.

To improve the fuel-air mixing, various external charge preparation devices such as a fuel vaporizer or a fuel atomizer[22−27] were also developed. Midlam-Mohler et al.[23] and Canova et al.[27] developed a fuel atomizer for achieving mixed mode HCCI/DI combustion in a single cylinder engine. They utilized the fuel atomizer up to medium engine loads but used direct fuel injection at higher engine loads. Puschmann et al.[26] prepared a homogeneous fuel-air mixture outside the engine combustion chamber using a "cool flame vaporizer". They carried out HCCI experiments and compared their results with other LTC strategies. They used simulation tools to investigate the effect of T_i on different LTC techniques. Ganesh and Nagarajan[24] developed a fuel vaporizer to prepare a homogeneous fuel-air mixture. The fuel vapors emitted from the fuel vaporizer formed light and dispersed aerosol, which has a negligible tendency of wall wetting. These tiny fuel droplets mix easily with the heated inlet air, resulting in formation of superior homogeneous charge. They did not use any external heating system to control the temperature of the fuel-air mixture, which resulted in the inferior fuel vaporizer performance at higher engine loads. Singh and Agarwal[28] also carried out HCCI experiments using a fuel vaporizer. They reported that enrichment of the fuel-air mixture leads to advanced combustion phasing and higher HRR. This was effectively controlled by EGR up to medium loads. Maurya and Agarwal[29] reported that the upper boundary of the HCCI combustion regime was limited by higher NOx emission, greater engine

knocking, and an unacceptably high noise level, which may potentially damage the engine. They also reported that a sharp increase in CO emissions defined the lower boundary of the HCCI operating regime (at low loads). At a lower engine load retarded combustion phasing increased cyclic variations due to engine misfiring. This happened due to a lack of thermal energy available for autoignition of the fuel-air mixture.[29−31] They suggested that the demand of thermal energy for the mixture's autoignition increased at lower engine loads; however, available thermal energy remained low in these conditions. Unavailability of adequate thermal energy for autoignition of the charge eventually leads to misfire. A lower boundary of the HCCI operating region was also sensitive to variations in T_i, which affected both the required thermal energy for autoignition of the charge and the heat transfer losses from the cylinder walls. When T_i decreased, the lower operating boundary moved up, and the HCCI operating regime shrank.[32] NOx formation depends on combustion phasing as well because the peak combustion chamber temperature increases at advanced combustion phasing. Agarwal et al.[33] reported that HCCI combustion resulted in significantly lower NOx emissions compared to conventional CI combustion, which could be further reduced by increasing the EGR. This reduction in NOx emissions was mainly due to slower chemical kinetics of the fuel-air mixture and retarded combustion phasing, which led to lower peak in-cylinder pressure and temperature. Asad et al.[34] suggested that HCCI combustion was predominantly chemical kinetics controlled hence combustion phasing was greatly affected by T_i. Higher T_i led to advanced combustion phasing, which resulted in higher NOx emissions, higher rate of pressure rise (RoPR), and higher in-cylinder pressure. They performed HCCI experiments at different T_i's and found that increased T_i with higher EGR quantities resulted in lower NOx and combustion phasing benefits.

Experimental studies have beyond reasonable doubt that HCCI combustion concept is advantageous because of its potential for very low NO_x and particulate emissions, which are usually close to negligible. Recent experimental investigations demonstrated that total particulate mass was indeed negligible, however significant number of particles in the size range below 100 nm mobility diameter were emitted in HCCI combustion, which could not be neglected.[35,36] Singh and Agarwal[34] performed HCCI experiments using different test fuels (mineral diesel, dieseline, diesohol and diesosene) to investigate the effect of fuel volatility on particulate emission characteristics. The experiments were carried out at constant EGR and T_i at different engine loads. They reported that particle number concentration was higher in ultrafine range; but slightly lower in the nanoparticle range for mineral diesel. Lower in-cylinder temperature with extremely lean operation prevented complete oxidation of boundary layer and crevice bound hydrocarbons, thereby increasing concentration of HC precursors, which enabled higher nucleation of particulate. The presence of large accumulation mode particles (AMP) for all test fuels was explained by the existence of diffusion burning. Franklin[37] investigated the effect of different HCCI control strategies on particulate emissions. Findings of this study strongly suggested that although HCCI combustion was free of AMP, nucleation mode particles (NMP) were present in significant mass and number in the exhaust of a fully premixed HCCI engine. Main source of precursors to these NMP primarily originated from volatile species of the lubricating oil. Abundance of volatile precursors and lack of adsorption and
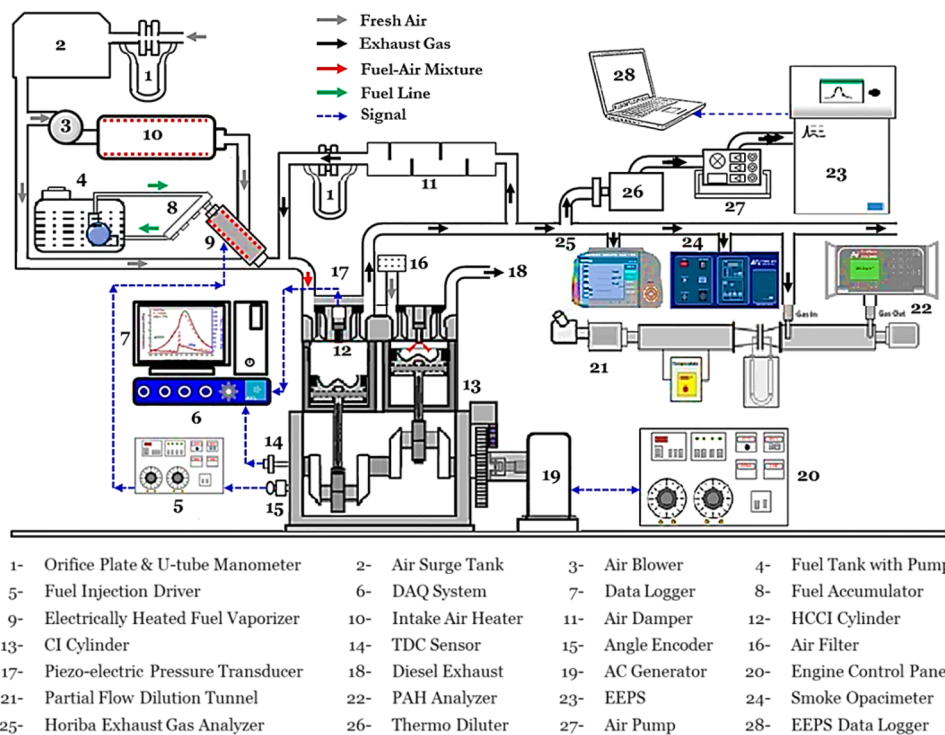
Figure 1. Schematic of the experimental setup for PHCCI combustion.

condensation sites in the combustion chamber created ideal conditions for homogeneous nucleation.[37] According to Kittelson,[38] carbonaceous agglomerates comprise of most of the particulate mass from diesel engines; however they can be significantly reduced by employing HCCI technology. They indicated that approximately 10% (w/w) of PM was inorganic, which primarily included trace metals and ash. Agarwal et al.[33] performed diesel HCCI experiments and investigated particulate emission characteristics at different relative air−fuel ratios (λ) and EGR rates. They reported that most diesel HCCI combustion generated particles were ultrafine particles. Particle number concentration increased with an increasing EGR rate. They suggested that increasing EGR rates and λ resulted in higher number of AMPs, which was mainly due to higher benzene soluble organic fraction (BSOF) of the PM. In another study carried out by Agarwal et al.,[39] effect of T_i on gasoline fueled HCCI combustion was also investigated. They reported that total particle number concentration increased with increasing T_i; however particulate numbers reduced in case of leaner fuel-air mixtures. Aceves and Flowers[40] reported that mineral diesel LTC exhibited low soot precursors at low EGR rates, but it increased rapidly as the EGR rate increased.

Although remarkable progress has been made in LTC technology, large-scale production of mineral diesel fueled HCCI engines for commercial applications still remains challenging and is affected by several operational difficulties. Therefore, the feasibility of mineral diesel fueled PHCCI combustion in a production grade engine has been explored in this study. This study was based on external charge preparation technique using a fuel vaporizer, which was thought to be a cost-effective solution for homogeneous fuel-air mixing. To explore the operating regime of PHCCI combustion, experiments were carried out in a wide range of engine loads. For better control over PHCCI combustion at extreme load conditions (rich and lean limits), experiments were performed

at different EGR rates and T_i's, and combustion, performance, emission and particulate characteristics of PHCCI engine were experimentally investigated.

2. EXPERIMENTAL SETUP

Experimental setup for PHCCI combustion can be divided into seven subsystems, namely (i) test engine, (ii) intake air heating system, (iii) EGR system, (iv) fuel vaporizer, (v) fuel injection system, (vi) data acquisition system, and (vii) emission measurement system. Schematic of experimental setup is shown in Figure 1.

2.1. Test Engine. Test engine used for PHCCI combustion investigation was a two-cylinder, four-stroke, constant speed, air-cooled direct injection diesel engine (Kirloskar; DA-16). The engine was coupled to a single phase, 11 kW, 220 V AC generator. A resistive load bank (10 kW capacity) was used for loading the engine-generator system. In the experimental setup, two separate fuel tanks were used for the fuel supply to the two cylinders of the engine. One cylinder of the engine was modified to operate in PHCCI combustion mode while the second cylinder was operated in conventional CI combustion mode. Compression ratio of PHCCI cylinder was reduced from to 16.5 from the original CR of 17.5. The intake and exhaust manifolds of PHCCI mode cylinder were decoupled from the manifold of CI mode cylinder. Detailed specifications of the engine with modified PHCCI cylinder and unmodified CI cylinder are given in Table 1.

For measurement of different engine related parameters such as temperature, speed, besides others, a set of instruments such as thermocouples, rpm sensors, temperature controller etc., were installed on the test engine at appropriate locations.

2.2. Intake Air Preheating System. PHCCI combustion experiments were performed in naturally aspirated (NA) engine. Volumetric intake air flow rate was measured using an orifice plate coupled to a U-tube manometer. To control the T_i, fresh air entering the fuel vaporizer was preheated using an electric air preheater (12 kW), which was installed downstream of the inlet surge tank. A blower was placed in between the surge tank and air preheater in order to induce the intake air into the fuel vaporizer via the preheater. The temperature of air supplied by the intake air preheater was controlled by a close-loop PID temperature controller. The heater controller took feedback from a thermocouple, which was installed downstream of the

**Table 1. Specifications of the Test Engine Used for PHCCI Combustion experiments**

engine characteristics	technical specifications	
	modified PHCCI cylinder	unmodified CI cylinder
make/model	ERL	Kirloskar/DA-16
fuel injection type	port injection	direct injection
fuel injection timing	450° bTDC	24° bTDC
fuel injection pressure	3 bar @ 1500 rpm	210 bar @ 1500 rpm
compression ratio	16.5:1	17.5:1
power output/cylinder	4.15 kW @ 1500 rpm	5.5 kW @ 1500 rpm
displacement per cylinder	770 cc	770 cc
bore/stroke	95/110 mm	
cooling system	air cooled	

preheater. Intake air could be preheated up to 250 °C with an accuracy of ±3 °C under steady state. In this study, intake air temperature T_i was varied between 160 to 200 °C.

2.3. Exhaust and EGR System. In order to control the HRR in the PHCCI cylinder, a fraction of exhaust gas was recirculated into the intake manifold. Exhaust gas was mixed with the partially homogeneous fuel-air mixture and fresh intake air, and then the mixture was supplied to the PHCCI cylinder during intake stroke. Therefore, exhaust manifold of the test engine was modified and a separate exhaust line was provided for the PHCCI cylinder. An EGR damper was used in the EGR loop to eliminate pressure pulsations. The EGR rate was regulated by a control valve, which was installed in the EGR line. This control valve connected the EGR damper to the exhaust line.

2.4. Fuel Injection System. The fuel injection system used in the PHCCI experimental setup consisted of an electric fuel pump (Denso; 1500M844M1), a fuel tank, a fuel accumulator, a fuel injector and an injector control circuit. An electrical fuel pump supplied fuel from the tank to the fuel accumulator under pressure. Fuel injector operates using 12 V TTL (transistor-transistor logic) pulse originating from the injector controller circuit. The schematic of the fuel injection system is given in Figure 2.

The fuel pump continuously supplied pressurized fuel to the fuel accumulator at 3 bar pressure. A 12 V electrical pulse actuated port fuel injector was used for the fuel injection. It was connected to the inlet of the fuel vaporizer. A fuel accumulator, which could be connected to three port fuel injectors, was modified to operate only
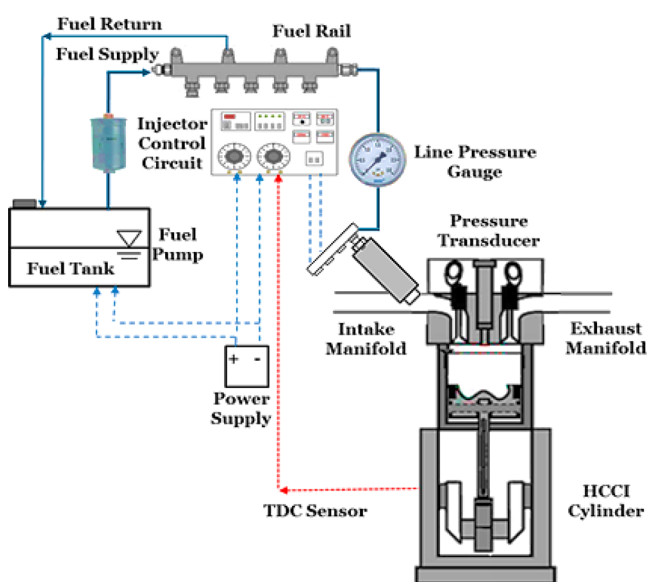
Figure 2. Schematic of the fuel injection system.

one fuel injector and the other two openings were blocked. A fuel injection timing circuit (driver circuit) was designed and fabricated, which generated the required TTL output that controlled the solenoid of the injector. Injector driver circuit took input of TDC signal and triggered the timing IC (IC555) for TTL output pulse generation. The cycle reference signal (TDC signal) was obtained from the engine using an inductive proximity sensor (Transducers and Allied Products, GLP18APS). This proximity sensor generated only one pulse per revolution of the crankshaft.

2.5. Fuel Vaporizer. Homogeneous fuel-air mixing is the most important requirement of LTC. Due to low volatility characteristics of mineral diesel like fuels, homogeneous mixture preparation remains a major obstacle in achieving LTC. In this study, a homogeneous fuel-air mixture was prepared using an external mixing device, referred to as a "fuel vaporizer". Schematic and photograph of the fuel vaporizer is shown in Figure 3. Main vaporizing chamber of the fuel vaporizer was made of aluminum. The MOC was chosen due to its high thermal conductivity and low reactivity with fuel-air mixtures. Cylindrical surfaces of the chamber were covered externally by a ceramic band heater, which heated it to enable fuel vaporization. Both sides of the main vaporizing chamber were fitted with connectors made of aluminum. At the inlet of the vaporizer, an arrangement for preheated intake air supply was made such that fuel vapors easily mixed with intake air in the intake manifold.

The cutoff temperature of the heater and the warm-up time were controlled using a voltage regulator. A thermocouple was installed at the outlet connector in order to control the fuel vaporizer temperature. Temperature of the electrical heater was controlled by the PID controller. Technical specifications of the fuel vaporizer are given in Table 2.

Liquid fuel was injected into the main vaporizer chamber using a solenoid port fuel injector. Heat supplied by the electric heater was absorbed by the atomized spray droplets, which eventually evaporated. Fuel vapors formed very light and dispersed aerosols, which followed the air motion. All properties of this "gas-like" aerosol made it suitable for external fuel-air mixture formation. High velocity intake air supplied by the air preheater forced the fuel vapors to mix with the intake air and formed a partially homogeneous fuel-air mixture. This mixture was then supplied to the combustion chamber through intake valve. The temperature of this homogeneous mixture was used as the intake charge temperature for PHCCI combustion mode.

2.6. In-Cylinder Data Acquisition System. In-cylinder pressure measurement was carried out using a piezoelectric pressure transducer (Kistler; 6013C). This pressure transducer was mounted flush on to the PHCCI cylinder head. An optical angle encoder (AVL; 365C) was used for crankshaft angle measurements. For in-cylinder pressure data acquisition and analysis, a compact combustion measurement system (AVL; IndiMicro) was used. An integrated Giga-bit Ethernet interface supported the real time raw data transfer to the PC using data acquisition software (AVL; IndiCom Mobile).

2.7. Emission Measurement System. For exhaust characterization, part of the exhaust gas from the PHCCI cylinder was supplied to an exhaust gas emission analyzer (Horiba; MEXA584L). This instrument is capable of measuring raw emissions of different gaseous species namely NO_x, HC, CO, and CO_2. Smoke opacity of the exhaust gas was measured by the smoke opacimeter (AVL; 437). For particulate characterization, an engine exhaust particle sizer (TSI; EEPS 3090) was used, which measured particle number-size distribution. EEPS can measure particles in the size range from 5.6 to 560 nm with a maximum concentration up to 10^8 particles/cm^3 of the exhaust gas. Therefore, exhaust gas was diluted using a rotating disc thermo-diluter, which diluted the exhaust gas 115 times. Concentration of polycyclic aromatic hydrocarbons (PAHs) in the engine exhaust was measured using an online PAH analyzer (Eco-Chem Laboratories; PAS 2000). This analyzer works on the principle of photoionization of particle-bound PAH's and is capable of real time measurement of particulate bound PAHs.
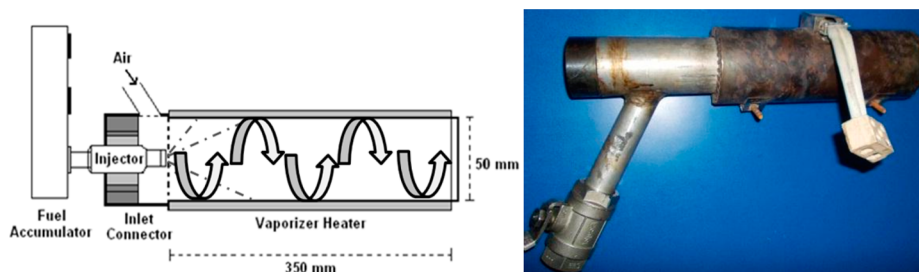
Figure 3. Schematic and photograph of the fuel vaporizer.

Table 2. Fuel Vaporizer Specifications

characteristics	specifications
heater power	1800 W
vaporizer diameter	50 mm
length of vaporizer	350 mm
warm-up duration	3 min

3. RESULTS AND DISCUSSION

First objective of this study was to explore the feasibility of mineral diesel fueled PHCCI combustion in a modified production grade engine. Second objective of this study was to investigate the effects of EGR and T_i on combustion, performance, emissions and particulate emission characteristics of a mineral diesel fueled PHCCI engine. Important properties of mineral diesel are given in Table 3.

Table 3. Important Properties of Mineral Diesel

property	mineral diesel
calorific value (MJ/kg)	43.54
density (g/cm³) @ 30 °C	0.831
viscosity (cSt) @ 40 °C	2.82
flash point (°C) (min.)	~54

Experiments were performed at constant engine speed (1500 rpm) at six different engine loads (λ = 1.5 to 5.25), three EGR rates (0, 10, and 20%) and three T_i's (160, 180, and 200 °C). PHCCI combustion was achieved over a wide range of λ (from 1.25−5.5). For selecting suitable range of PHCCI combustion, two parameters namely: coefficient of variation (COV) of indicated mean effective pressure (IMEP) (COV_{IMEP}) and maximum rate of pressure rise (R_{max}) were used. COV_{IMEP} was used to define the lower limit of engine operating range and showed combustion stability of the PHCCI engine. COV_{IMEP} was calculated from IMEP data of 1000 consecutive engine cycles. Results obtained showed that COV_{IMEP} reduced with decreasing λ and higher COV_{IMEP} were attained at relatively leaner fuel-air mixtures. For λ > 5.25, stable combustion could not be achieved due to higher COV_{IMEP}. This was due to excessive misfiring. Therefore, λ = 5.25 was selected as the misfire limit (lean limit, with COV_{IMEP} > 4%) for PHCCI experiments. Similarly, R_{max} was used to define the upper limit of the PHCCI combustion. R_{max} increased with decreasing λ and fuel-air mixtures richer than λ = 1.5 resulted in erratic and noisy combustion due to unacceptably high R_{max}. Therefore, λ = 1.5 was selected as the knocking limit (rich limit, $R_{max} \geq 25$ bar/CAD) for PHCCI experiments. In between these two limits, experiments were performed at six different engine loads. These loads were classified into three load ranges namely

higher engine loads (λ = 1.5 to 2.25), medium engine loads (λ = 3.0 and 3.75) and lower engine loads (λ = 4.5 and 5.25).

Results of PHCCI combustion are divided into four categories, namely combustion, performance, emission and particulate characteristics and are described in the sections given below.

3.1. Combustion Characteristics. In-cylinder pressure variations w.r.t. crank angle position is an important parameter used in combustion analysis. The in-cylinder pressure was measured using a piezoelectric pressure transducer and crank angle position was measured using an angle encoder with a resolution of 0.1 CAD. For all experimental conditions, in-cylinder pressure data and derived parameters such as HRR, start of combustion (SoC), combustion duration, etc., were analyzed for an average of 250 consecutive engine cycles.

In Figures 4a-r, variation of in-cylinder pressure at different engine loads, T_i's, and EGR rates were compared vis-à-vis the motoring curve (i.e., in-cylinder pressure without combustion). This figure showed that the maximum in-cylinder pressure (P_{max}) corresponded to the richest fuel-air mixture (λ = 1.5) (Figures 4a-c) and the lowest P_{max} corresponded to the leanest fuel-air mixture (λ = 5.25) (Figures 4p-r). P_{max} decreased with increasing λ because lesser fuel quantity was supplied to the combustion chamber through the fuel vaporizer for formation of leaner fuel-air mixtures.

Deviation of the in-cylinder pressure curve from the motoring curve showed SoC. With increasing engine load (from λ = 5.25 to 1.5), SoC shifted toward bTDC (~5 to 15 CAD) (Figures 4a, d, g, j, m, and p). This was mainly due to the presence of relatively higher fuel quantity in the fuel-air mixture, which enhanced fuel-air mixture reactivity and resulted in faster combustion. Earlier SoC of relatively richer fuel-air mixture also resulted in advanced crank angle positions of P_{max} (Figures 4a-c). Richer mixtures (lower λ) showed steeper pressure rise, which led to unacceptable combustion noise due to knocking (Figures 4a-c). For very lean fuel-air mixtures, misfire during PHCCI increased, which led to retarded combustion phasing and relatively lower P_{max}. At all T_i's and EGR rates, λ = 1.5 showed erratic behavior due to excessive knocking (Figures 4 a-c). A slightly inferior performance of the fuel vaporizer due to the presence of higher fuel quantity was attributed as the reason for this behavior, which led to mixture heterogeneity. This trend was also reported by Singh and Agarwal.[34] They added volatile additives in mineral diesel to improve the fuel vaporizer's performance. At λ = 5.25, SoC retarded due to longer ignition delay (Figures 4p-r). This was followed by slower combustion, resulting in lower P_{max}.[23,24]

For a constant λ, increasing T_i resulted in relatively higher P_{max} due to improved fuel vaporization. Higher P_{max} led to higher in-cylinder temperatures, which resulted in relatively earlier autoignition and advanced combustion phasing. With
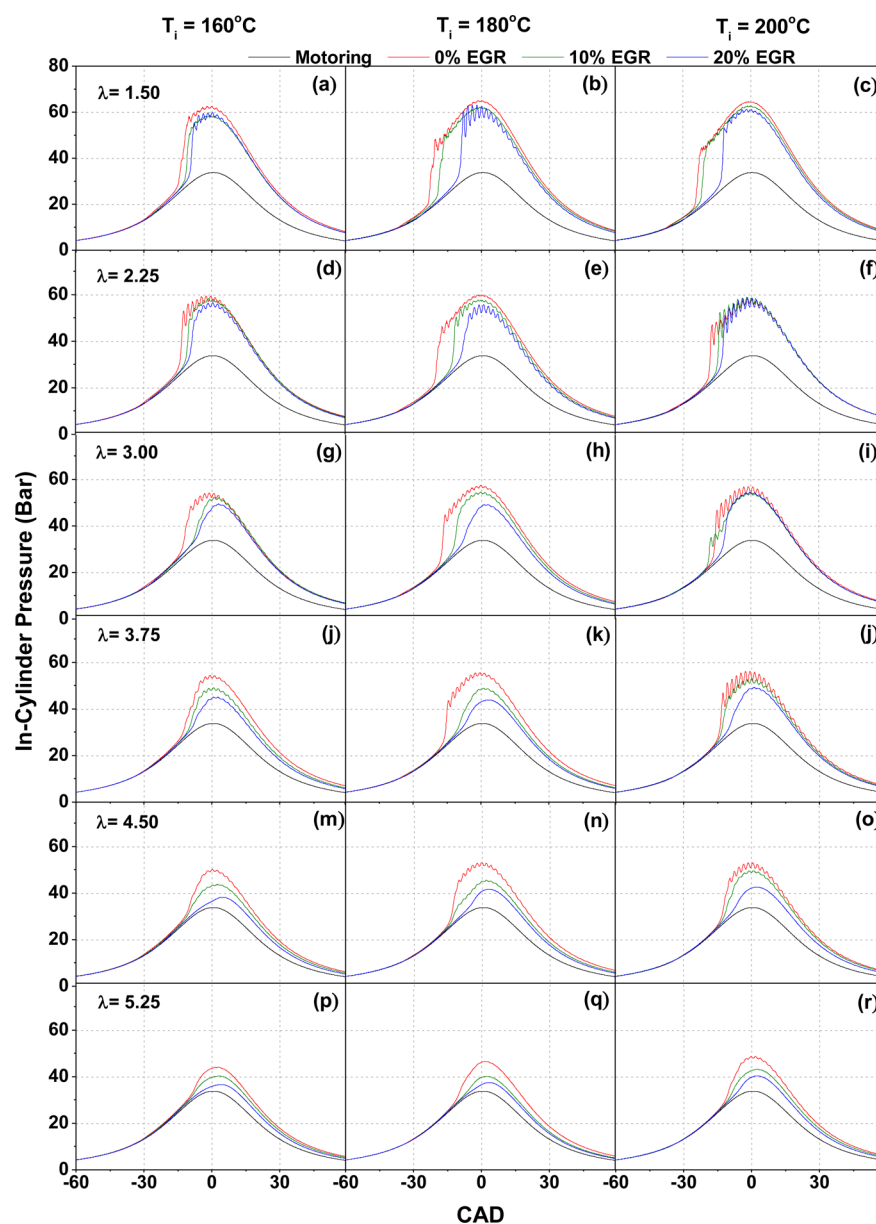
Figure 4. Variation of in-cylinder pressure in case of mineral diesel fueled PHCCI engine at different loads, T_i's, and EGR rates.

increasing T_i, improvement in combustion behavior at low engine loads could be observed (Figures 4n, o, q, and r). Higher T_i improved the combustion kinetics of fuel-air mixtures and resulted in relatively earlier SoC. At medium engine loads (λ = 3.0 and 3.75, Figures 4 g-l), combustion significantly improved by increasing T_i; however, it resulted in higher knocking at relatively higher engine loads (Figures 4c, f, i, and j). Similar trends were reported by Singh and Agarwal.[36] Comparison of in-cylinder pressure curves at higher engine loads (λ = 1.5 and 2.25) and T_i showed that 10% EGR rate improved combustion and resulted in 1 to 3 bar higher in-cylinder pressure (Figures 4a, b, d, and e). However, at all engine loads and T_i, 20% EGR rate reduced mixture reactivity, resulting in retarded SoC and lower P_{max} (Figures 4). EGR was found to be more effective at higher engine loads (λ = 1.5 and 2.25, Figures 4 a-f) and T_i. Midlam-Mohler et al.[23] also reported similar trends. However, at lower engine loads (λ = 4.5 and 5.25, Figures 4 m-r), EGR was less sensitive to PHCCI combustion due to lower in-cylinder temperatures. At higher T_i,

EGR controlled SoC and knocking, thus EGR could be used as the main control parameter in LTC.

Figures 5a-r show the variation of HRR at different engine loads, T_i's, and EGR rates. HRR was calculated from the acquired cylinder pressure data using the "zero dimensional heat release model".[41] HRR is a measure of rapidness of chemical energy conversion into thermal energy during combustion. HRR patterns were found to be significantly different compared to conventional combustion modes. In PHCCI combustion, HRR_{max} reached ~275 J/CAD (Figures 5c and f), which was mainly due to specific volumetric combustion phenomena. The magnitude of HRR_{max} was significantly higher compared to values reported by Ganesh and Nagarajan.[24] This showed that intake air heating improved fuel vaporization and resulted in a superior homogeneous fuel-air mixture. Simultaneous autoignition of the fuel-air mixture inside the combustion chamber was the main reason for higher HRR, which resulted in volumetric combustion. HRR during PHCCI combustion reduced with decreasing engine load. For richer mixtures, a
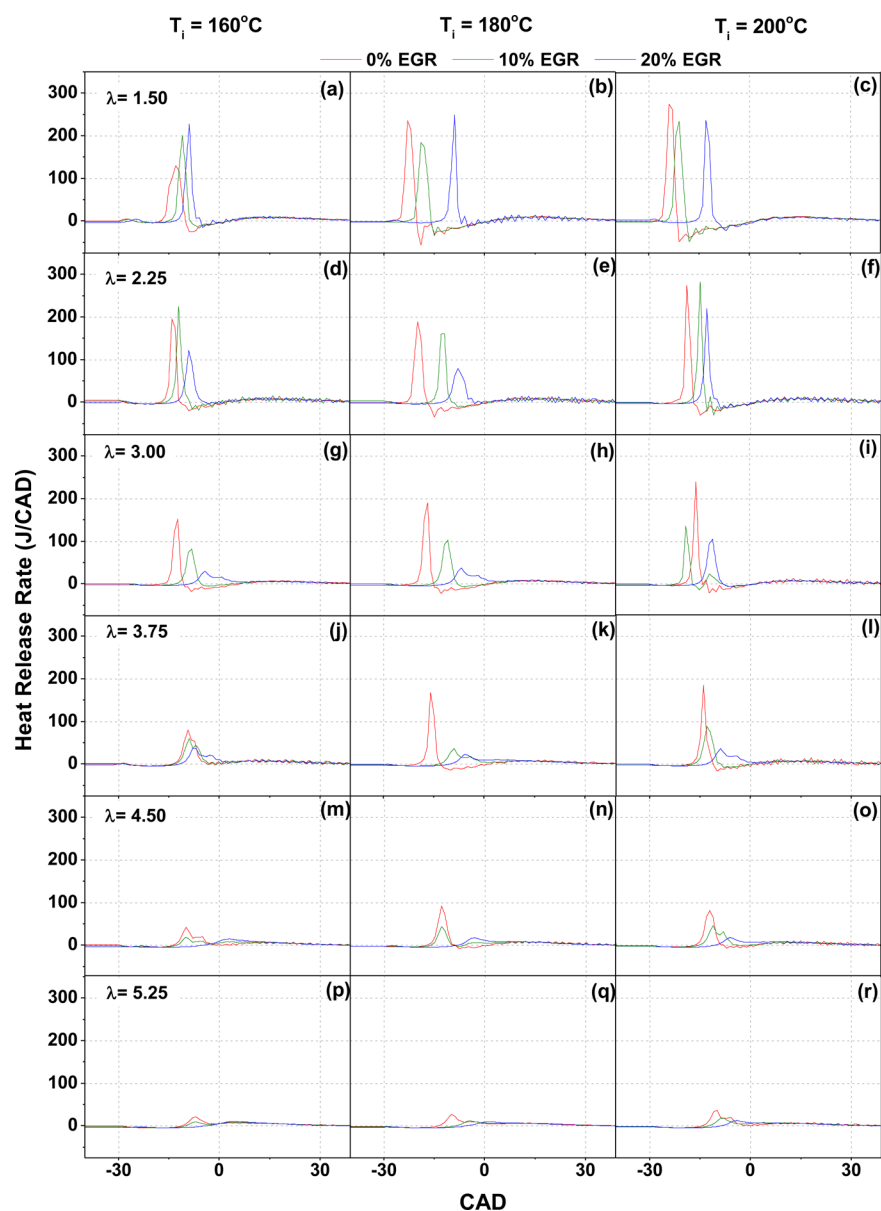
Figure 5. HRR of the diesel fueled PHCCI engine at different loads, T_i's, and EGR rates.

larger fuel quantity autoignited at several combustion chamber locations compared to leaner mixtures; therefore, HRR was relatively higher in the case of richer fuel-air mixtures.

When mixtures were very lean, the probability of engine misfire increased (λ = 4.5 to 5.25) (Figures 5 m-r), and combustion phasing was too late, resulting in lower HRR. As mixtures became richer, combustion phasing advanced, and decreasing λ (from 3.0 to 1.5) (Figures 5a-i) caused an increase in peak HRR. At λ = 1.5, HRR showed random behavior due to excessive knocking. At other engine loads (λ = 2.25 to 5.25) (Figures 5 d-r), HRR decreased with an increasing EGR rate (Figures 5 a-r). Energy absorbed by high heat capacity species of exhaust gas and slower chemical kinetics were the main reasons for relatively lower HRR at higher EGR rates. This trend was similar to the observation of Ganesh and Nagarajan.[24] Due to intake air heating, relatively lesser effectiveness of EGR at lower engine loads can be clearly seen from the trends of HRR (Figures 5m-r). These trends were different from previously reported trends.[34] Figures 5a-r

showed that HRR increased with increasing T_i. At higher T_i, the combustion chamber temperature increased, which resulted in faster reaction kinetics, leading to relatively earlier autoignition. Also at higher T_i, fuel-air mixing also improved, which enhanced the degree of completeness of combustion thus resulting in higher HRR.[36] The width of the HRR curve decreased with increasing T_i, which showed shorter combustion duration of PHCCI combustion due to faster fuel-air chemical kinetics.

Figures 6a-c show the variation of R_{max}, knock integral (KI) (Figures 6d-f), knock peak (KP) (Figures 6g-i), and combustion noise (Figures 6j-l) at different engine loads, T_i's, and EGR rates. R_{max} was used to define the upper limit of the PHCCI operating range and was controlled by premixed heat release. KI represented the integral of superimposed rectified knock oscillations, and KP reflected the absolute maxima of the rectified knock oscillations superimposed on the cylinder pressure curve. Knocking parameters were determined from pressure signals, which were filtered through a high pass filter
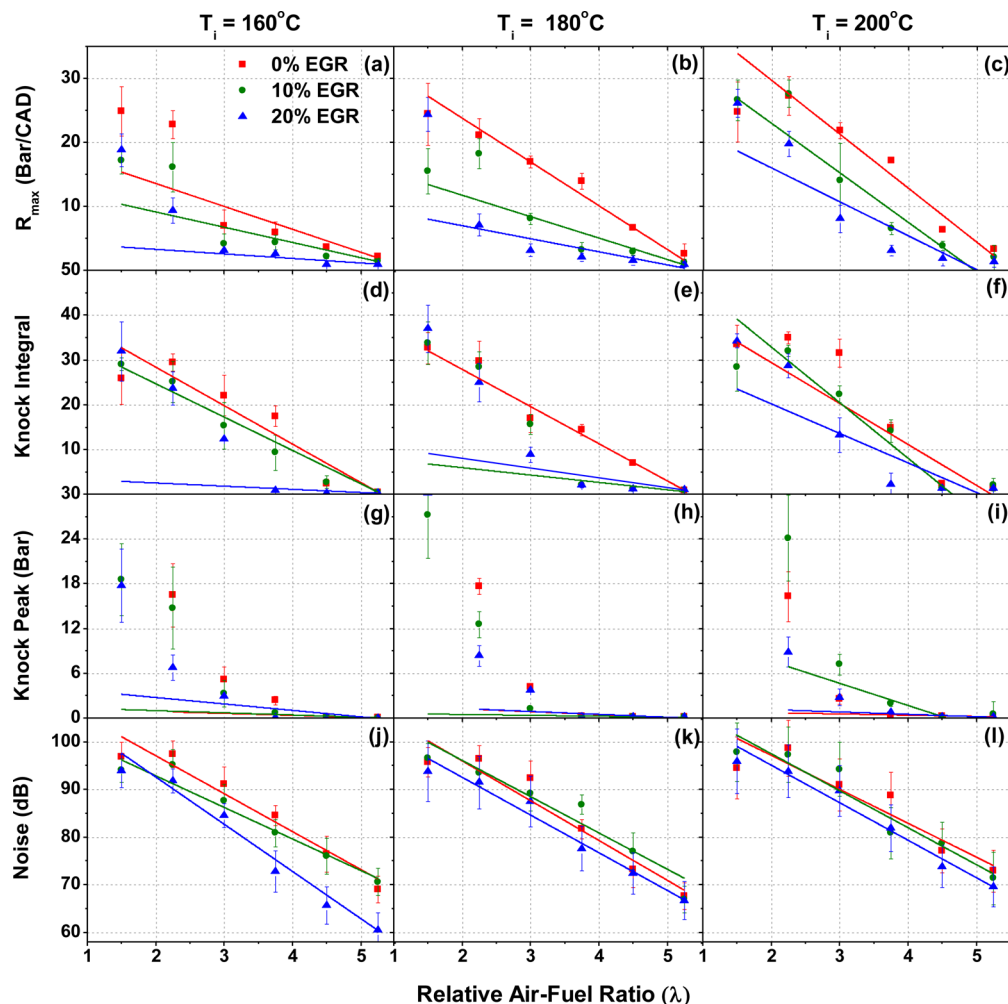
Figure 6. R_{max}, KI, KP, and combustion noise of the mineral diesel fueled PHCCI engine at different loads, T_i's, and EGR rates.

and then rectified. Parameters such as KI or KP of the superimposed oscillations were determined from the measured signals. The noise level was calculated from the cylinder pressure signals.[41]

From Figures 6a-c, it can be seen that R_{max} increased with increasing engine load. At $\lambda = 1.5$, R_{max} reached up to ~30 bar/CAD; therefore, PHCCI experiments were limited up to this load. R_{max} decreased with an increasing EGR rate, whereas increasing T_i resulted in higher R_{max}. Increasing T_i promoted chemical kinetics of fuel-air mixtures, resulting in faster combustion and consequently higher R_{max} (Figures 6a-c). Slopes of the trend lines of R_{max}, which is a measure of combustion rapidness, were also affected by T_i and the EGR rate. It increased with increasing T_i but decreased with an increasing EGR rate (Figures 6a-c).

In-cylinder knocking and noise were directly influenced by HRR, which was affected by parameters such as fuel quantity, in-cylinder temperature, fuel cetane number, and combustion efficiency. Noise could be directly correlated with knocking, because it is produced mainly due to late shockwaves inside the combustion chamber, which is generated by late combustion phasing. Increasing fuel quantity inside the combustion chamber resulted in faster fuel-air chemical kinetics, resulting in higher KI (due to severity of detonation). This could potentially damage the engine and lead to unacceptably high NOx emission levels. KI was less sensitive to T_i; however,

application of a high EGR rate (20%) reduced KI significantly. At lower engine loads, KI was found to be almost negligible (Figures 6d-f). KP followed a random trend as KP was very high at higher engine loads. These KP trends justified the non-applicability of PHCCI combustion at high engine loads. At lower engine loads, KP was ~0 bar, which was also visible from the in-cylinder pressure curves (Figure 4). Combustion noise results showed that in-cylinder combustion noise increased with increasing engine load. At higher engine loads, noise levels increased up to 100 dB (Figures 6j-l). Use of EGR reduced combustion noise. At 10% EGR rate, combustion noise was almost similar to no EGR condition, but at 20% EGR rate, combustion noise reduced by ~5 dB compared to no EGR.

Using mass fraction burned (MFB) analysis, variation in SoC, combustion phasing, and combustion duration at different engine loads, T_i's, and EGR rates are shown in Figure 7. Crank angle position corresponding to 10% CHR (CA_{10}) was used as SoC. In the experiment, SoC was significantly affected by the engine load, T_i, and EGR rate (Figures 7a-c). With increasing T_i, SoC advanced; however, application of EGR retarded the SoC. At higher T_i, improved fuel vaporization resulted in a relatively shorter ignition delay (Figures 7b-c). EGR hampered the chemical kinetics of the fuel-air mixture therefore retarding the SoC.

Crank angle position corresponding to 50% CHR (CA_{50}) was used as combustion phasing, which is a measure of overall
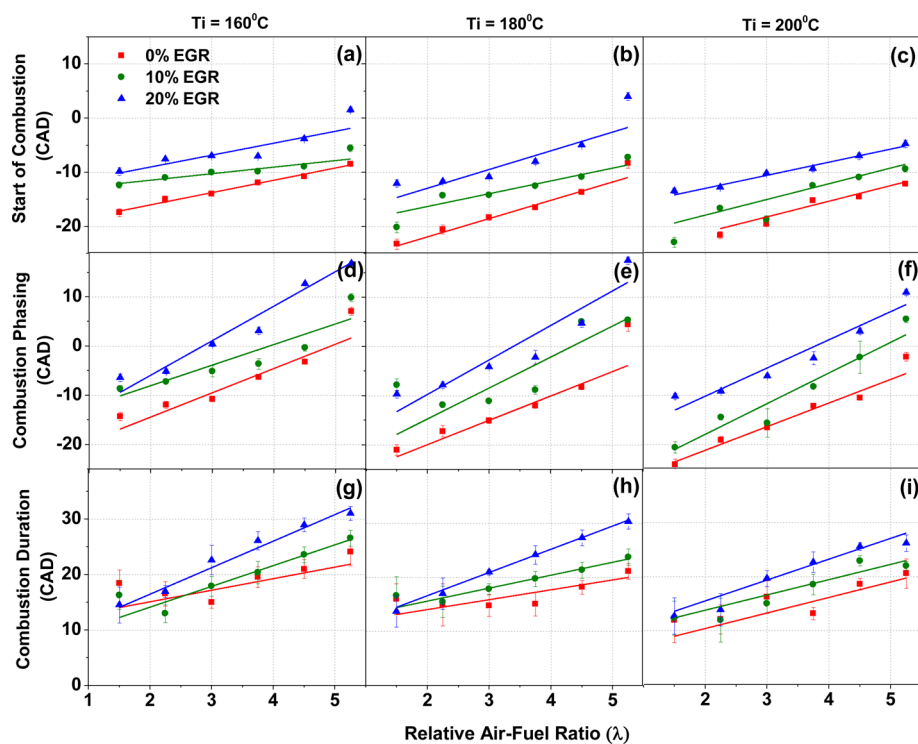
Figure 7. SoC, combustion phasing, and combustion duration of mineral diesel fueled PHCCI engine at different loads, T_i's, and EGR rates.
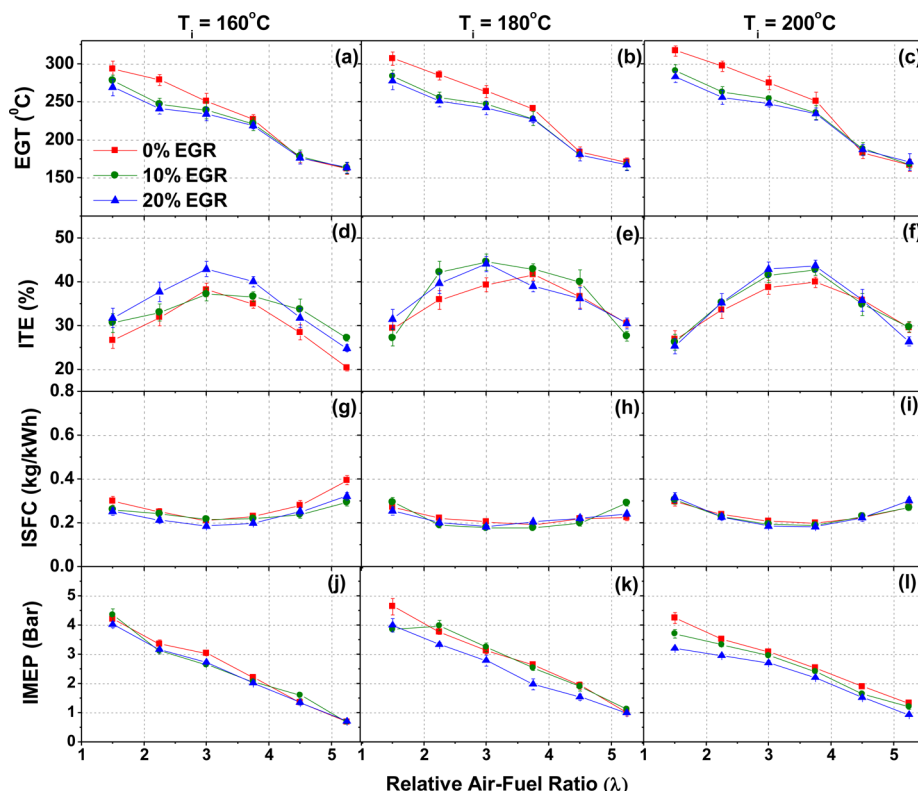

Figure 8. EGT, ITE, ISFC, and IMEP of the mineral diesel fueled PHCCI engine at different loads, T_i's, and EGR rates.

combustion during an engine cycle. Very advanced combustion phasing resulted in lower combustion efficiency due to a steep rise in the in-cylinder pressure, leading to higher HRR and in-cylinder temperature. This increased the heat transfer losses from the cylinder walls and the piston, which eventually reduced the work done on the piston by the expanding gases.

Too late combustion phasing resulted in lower in-cylinder temperature. This in turn increased emissions of HC and CO with reduced combustion efficiency. Optimum combustion timing varied with engine load, T_i, and EGR. With increasing engine load, combustion phasing advanced, whereas combustion phasing retarded at lower engine loads (Figures 7d-f). At
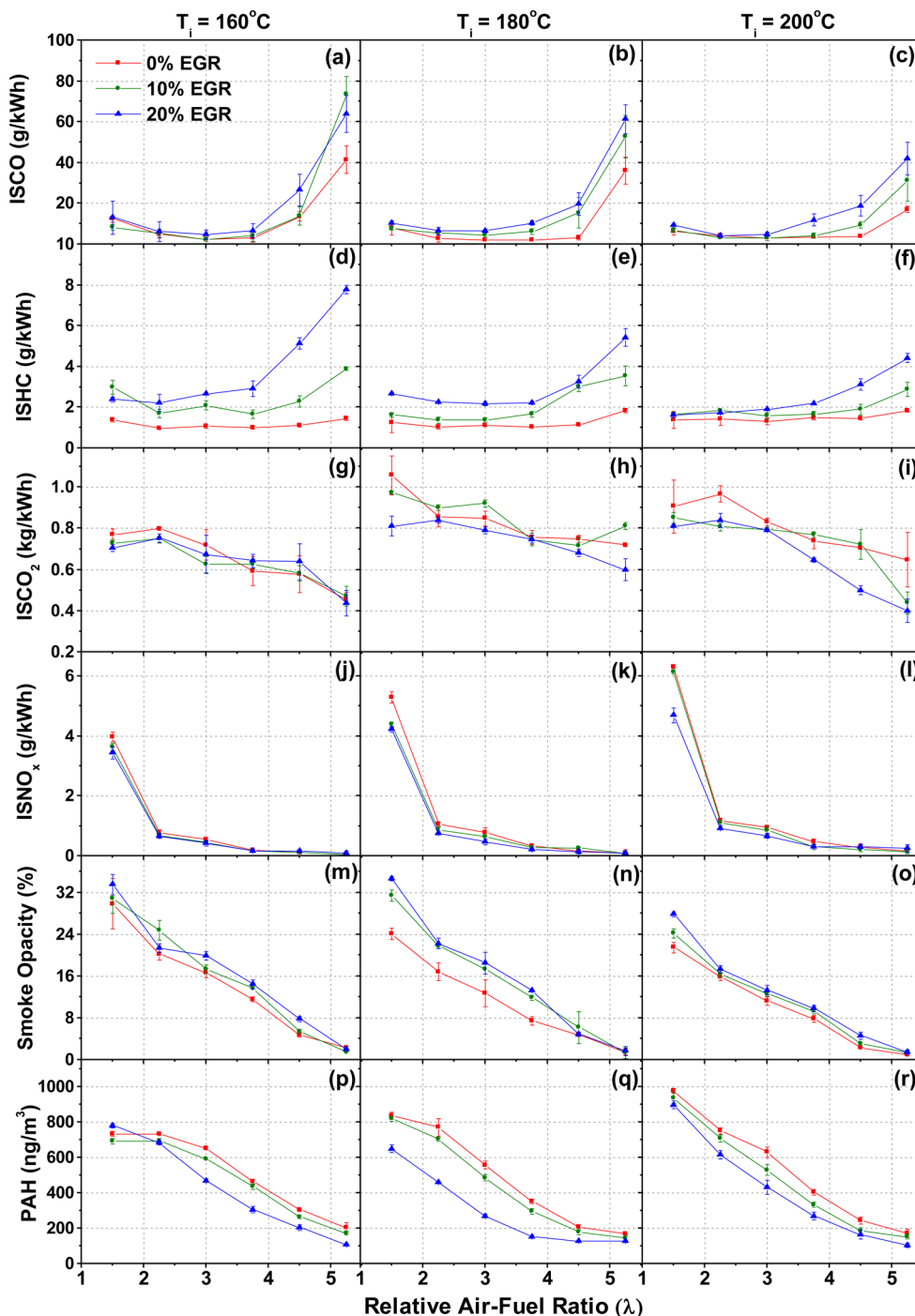
Figure 9. ISCO, ISHC, ICCO$_2$, ISNO$_x$, smoke opacity, and PAH emissions from mineral diesel fueled PHCCI engine at different loads, T_i's, and EGR rates.

lower engine loads, fuel flow rate decreased and PHCCI combustion became slower, resulting in retarded combustion phasing. This reduced in-cylinder pressure and temperature and ultimately increased cyclic variations since autoignition was dependent on in-cylinder pressure and temperature to initiate the chemical reactions. At medium engine loads, combustion phasing was optimum, resulting in stable PHCCI combustion and optimum engine performance. With an increasing EGR rate, combustion phasing retarded which was beneficial at higher engine loads (Figures 6d-f). Similarly increasing T_i led to advanced combustion phasing with relatively improved combustion characteristics at low engine loads (Figures 7e

and f). This advanced combustion phasing was due to earlier SoC caused by higher initial charge temperature. Combustion phasing advanced (∼20 to 30 CAD) with increasing engine load. Figures 7a-f showed that SoC timing was strongly related to combustion phasing with variation in T_i. At higher T_i, combustion phasing advanced and followed a trend very similar to SoC (Figures 7a-f).

Crank angle position corresponding to 90% CHR (CA$_{90}$) was used as the end of combustion (EoC). Using the difference in EoC and SoC, combustion duration was calculated. PHCCI combustion showed relatively shorter combustion duration due to volumetric combustion inside the combustion chamber. For

all experimental test conditions, combustion duration increased with increasing engine load (Figures 7g-i). This was mainly due to the presence of higher fuel quantity, which led to relatively inferior fuel vaporizer performance. Combustion duration increased with an increasing EGR rate; however, higher T_i showed relatively shorter combustion duration. The main reason behind longer combustion duration at a higher EGR rate was slower combustion rate, due to two factors. The first factor was availability of a relatively lesser fuel quantity in the combustion chamber, and the second factor was dilution of the fuel-air mixture by the EGR. Comparison of trends of SoC and combustion duration showed that combustion duration increased with retarded SoC timings (Figures 6a-c and g-i). Relatively slower combustion was attributed mainly to lower average combustion temperature. For retarded SoC, gas expansion before transition to the high temperature oxidation during combustion further reduced the combustion chamber temperature. This in turn further reduced the combustion rate. Initially slow combustion rate delayed the temperature rise, and lower peak temperature was attained due to further expansion of charge because of piston movement. Combustion duration also increased due to increased temperature distribution in the charge volume, which further reduced the rate of combustion.

3.2. Performance Characteristics. Figure 8 shows the variations in engine performance parameters such as exhaust gas temperature (EGT), indicated thermal efficiency (ITE), indicated specific fuel consumption (ISFC), indicated specific energy consumption (ISEC), and IMEP at different engine loads, T_i's, and EGR rates. For engine performance analysis, all parameters were analyzed for their indicated values, which were based on in-cylinder pressure measurements. Here engine load was expressed as IMEP, which is a valuable measure of an engine's capacity to do work, independent of its size.

EGT (Figures 8a-c) was used as an approximate measure of in-cylinder combustion temperature because EGT depends on both in-cylinder combustion and combustion phasing. In PHCCI combustion, EGT is mainly controlled by the premixed combustion due to the absence of diffusion combustion phase. This resulted in significantly lower EGT from PHCCI combustion compared to conventional CI combustion, which also led to relatively lower NOx emission. For the richest fuel-air mixtures, EGT reached up to ~325 °C (Figure 8c), and for the leanest fuel-air mixture condition, maximum EGT was limited to ~175 °C (Figure 8a). EGT reduced with decreasing engine load. The presence of lesser fuel quantity in the engine combustion chamber and relatively lower in-cylinder temperatures were the main reasons for such a trend.

EGT also decreased with an increasing EGR rate. At higher EGR rates, higher heat capacity of exhaust gas species such as CO_2, H_2O, etc. absorbed more combustion generated heat, resulting in relatively lower EGT. At high engine loads, the difference in EGT at 0 and 10% EGR rates was large; however, it decreased at lower engine loads. This showed that EGR was relatively less effective at lower engine loads. Relatively higher EGT at higher T_i was another important observation. At higher T_i, combustion improved due to the faster combustion chemistry of fuel-air mixtures, which led to higher in-cylinder temperatures thus increased EGT.

ITE was mainly dependent on combustion efficiency and combustion phasing (Figures 8d-f). The ITE trend showed that combustion improved at medium engine loads (λ = 2.25 to 3.00), and combustion efficiency was relatively inferior at low engine loads (λ = 3.75 to 5.25). Further, ITE increased with

increasing engine load, reaching a maxima and then decreased. ITE decreased at very high engine loads due to higher knocking, which enhanced the rate of heat transfer. At higher engine loads, ITE improved with an increasing EGR rate due to controlled PHCCI combustion. An increasing EGR rate at high engine loads shifted the combustion toward the TDC, which reduced the negative compression work. ITE was also affected by T_i. At higher T_i, ITE improved due to optimized combustion phasing. At very high T_i, too advanced combustion phasing decreased ITE, and application of EGR retarded the combustion phasing, which resulted in relatively higher ITE (compared to no EGR condition) (Figure 8f). Figure 8 showed that ITE could be optimized by selecting suitable T_i and an EGR rate. ISFC decreased with increasing engine load. At higher engine loads, ITE improved, which resulted in relatively lower ISFC (Figures 8g-i). Application of higher T_i and EGR further improved ISFC. Using higher T_i and EGR, combustion phasing shifted into the optimum range, which resulted in more power output at relatively lower specific fuel consumption. Figures 8j-l showed that IMEP decreased for leaner fuel-air mixtures due to lower heat release in the combustion chamber. IMEP increased with increasing T_i (up to 180 °C); beyond which a further increase in T_i resulted in relatively lower IMEP. The EGR rate also affected IMEP which reduced with an increasing EGR rate. These variations in IMEP were closely related to combustion phasing. At very late combustion phasing (low engine loads and high EGR rates), temperature inside the combustion chamber was lower, leading to incomplete combustion. Therefore, a significant amount of fuel was emitted in the form of HCs, and combustion efficiency was relatively lower, leading to lower IMEP. IMEP increased at advanced combustion phasing. However, with too advanced combustion phasing (high engine loads and T_i), increased knocking enhanced the heat transfer to the piston and cylinder walls, resulting in lower IMEP.

3.3. Emission Characteristics. Figure 9 shows the emission characteristics of the mineral diesel fueled PHCCI engine. Gaseous emissions are presented in indicated specific (IS) values. ISCO emissions first decreased and then slightly increased with increasing engine load (Figures 9a-c). This was due to relatively higher in-cylinder temperature at higher engine loads, which promoted conversion of CO into CO_2. At higher engine loads, ISCO emissions increased due to lower availability of oxygen in the cylinder, which prevented conversion of CO into CO_2. Employment of EGR increased the ISCO emission due to relatively lower peak in-cylinder temperatures. These trends were similar to the results reported by Asad et al.[34] Reduction in ISCO emission with increasing T_i was an important observation, which was useful at lower engine loads. ISHC emissions followed a similar trend as ISCO; however, the effect of EGR and T_i was relatively stronger compared to that of ISCO (Figures 9d-f). $ISCO_2$ slightly increased with increasing engine load due to the presence of higher fuel quantity in the combustion chamber at higher engine loads (Figures 9g-i). Better conversion kinetics of CO to CO_2 at higher engine loads was another important reason for higher CO_2 emission. This conversion efficiency further improved with increasing T_i. Application of EGR resulted in an irregular behavior of $ISCO_2$ and was attributed to relative dominance of CO_2 concentration (ppm) and engine power output. In general, a higher EGR rate resulted in lower CO_2 concentration due to relatively lesser fuel quantity requirement and lower in-cylinder temperatures.
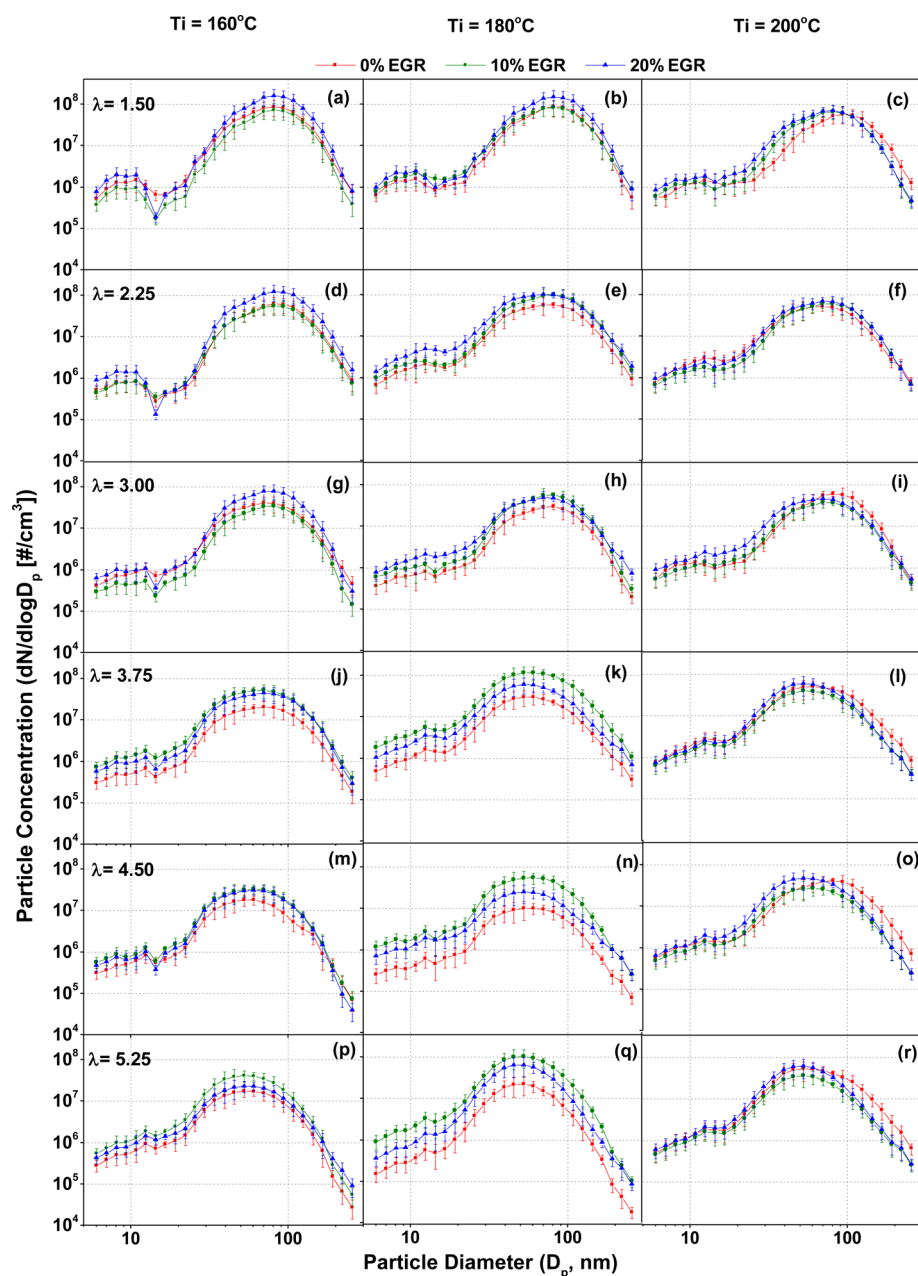
Figure 10. Number-size distribution of particulate emitted by mineral diesel fueled PHCCI engine at different loads, T_i's, and EGR rates.

ISNOx was very low for PHCCI combustion (Figures 9j-l). It was observed that NOx emissions were the highest for richer fuel-air mixtures, closer to the knock limit regime and lowest for leaner fuel-air mixtures, closer to the misfire regime. This was due to in-cylinder combustion temperature, which was higher for richer and lower for leaner fuel-air mixtures. Many researchers have demonstrated that the NOx formation rate increased exponentially with increasing in-cylinder temperature.[29,31] At temperatures above 1800 K, the NOx formation rate increased rapidly.

In PHCCI combustion, a strong correlation between NOx emissions and combustion phasing was another important observation (Figures 7d-f and 9j-l). NOx emissions were higher for advanced combustion phasing. Combustion chamber temperature increased with advanced combustion phasing due to earlier ignition and higher T_i, which resulted in higher NOx formation. Asad et al.[34] carried out similar experiments at lower

T_i's and reported similar observations. Smoke opacity increased with an increasing engine load and EGR rate. Smoke opacity at higher engine loads was slightly higher compared to the values reported by other researchers.[39] At higher engine loads, higher fuel quantity was injected in the main vaporizing chamber of the fuel vaporizer, which resulted in a slightly inferior vaporizer performance. This led to formation of heterogeneous fuel-air mixtures and resulted in higher smoke opacity at higher engine loads.[33] Results showed that the performance of the fuel vaporizer improved at higher T_i, which led to relatively lower smoke opacity compared to the one at lower T_i. An increasing EGR rate resulted in higher smoke opacity due to reduction in corresponding peak in-cylinder temperatures.

Particulate bound PAHs were also measured at different engine loads, EGR rates, and T_i's. Although PAHs are unregulated pollutants, they are extremely harmful to human health. Some of the PAHs are already recognized as being
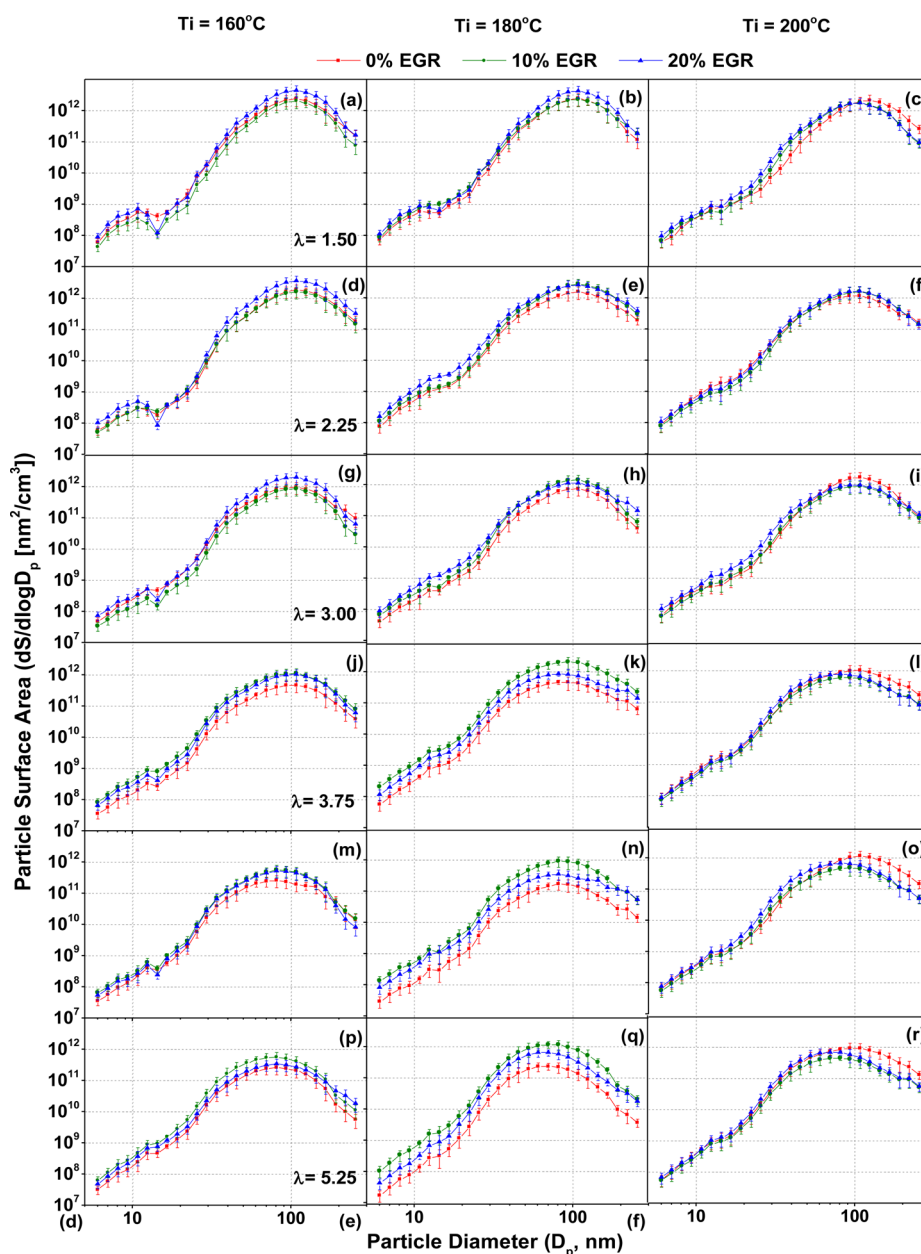
Figure 11. Surface area-size distribution of particulates emitted by mineral diesel fueled PHCCI engine at different loads, T_i's, and EGR rates.

"carcinogenic", which led to an increased human morbidity and mortality rates. PAHs measurement was important for PHCCI combustion because these compounds were produced mainly due to pyrolysis and structural modifications of the unburned fuel molecules, which were relatively higher in the PHCCI combustion. Results showed that PAH emissions increased drastically as the fuel-air mixtures became richer. Studies by other researchers have reported that HCCI combustion at higher engine loads resulted in higher PAH emissions.[35] Increasing T_i also resulted in slightly increased PAH emissions. Comparison of combustion phasing and PAH emissions showed a direct correlation between them. PAH emissions increased with advancing combustion phasing. Among all experimental conditions, maximum PAH emissions were ~1000 ng/m³ (at $\lambda = 1.5$, $T_i = 200$ °C, and EGR = 0%) with the minimum emissions of ~100 ng/m³ (at $\lambda = 5.25$, $T_i = 160$ °C, and EGR = 30%).

3.4. Particulate Emission Characteristics. Different researchers have demonstrated that particulate emissions from HCCI engine cannot be neglected.[33,37,38] Various factors, namely piston and wall wetting, charge heterogeneity, condensation of volatile species, nucleation, and ash and trace metals, affect particulate emissions from HCCI engines. Improved mixture preparation in the HCCI engine was suggested as the most important parameter for reducing the particulate formation due to reduction in solid carbon condensation sites.[33] Therefore, particulate measurement was carried out to investigate the effect of T_i's and EGR on fuel-air mixture homogeneity. In order to characterize particulate emissions in PHCCI combustion, experiments were performed at different engine loads, EGR rates, and T_i's with results presented as total particle numbers and mass and surface area distributions w.r.t. particulate size.

Figure 10 shows the particle number-size distribution of mineral diesel PHCCI at different operating conditions. Results
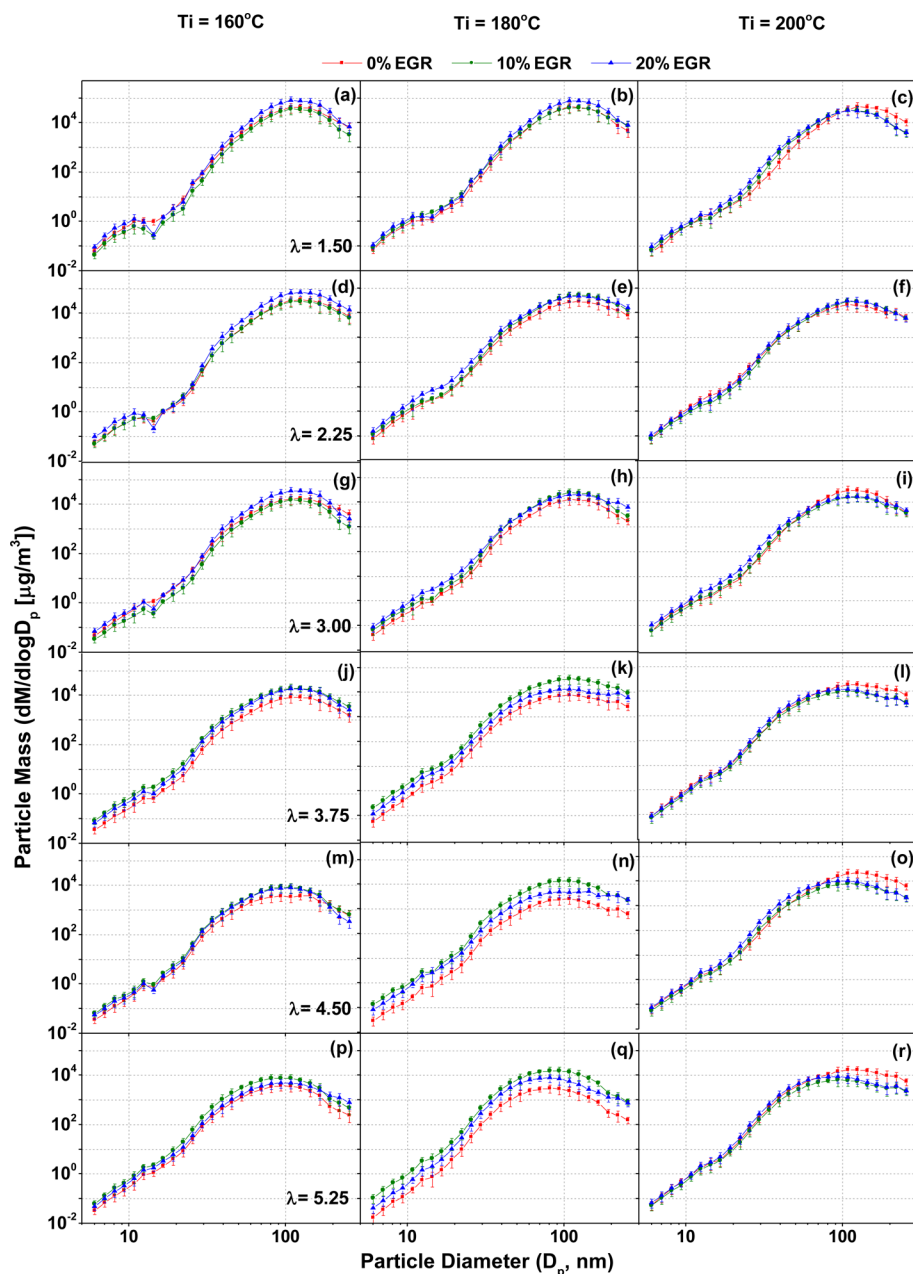
Figure 12. Mass-size distribution of particulates emitted by mineral diesel fueled PHCCI engine different loads, T_i's, and EGR rates.

are presented as log−log plots due to data spans covering several orders of magnitude.

Particulate results showed an important observation that despite large differences in combustion results with different loads, EGR rates, and T_i's, particulate results were quite comparable with these variables. From particle number-size distribution, it can be observed that nanoparticles ($D_p < 10$ nm) were also present in PHCCI exhaust (Figure 10a, d, g, and j), and their concentration (~10^6 particles/cm^3) significantly contributed to the total particle number concentration (Figure 13g). Concentration of particles with size greater than 200 nm was very low compared to relatively smaller particles. Results showed that particle number concentration increased with increasing engine load. With increasing engine load, λ decreased, and relatively richer fuel-air mixtures in the combustion chamber favored soot formation and particulate agglomeration. The presence of higher fuel quantity led to

formation of a larger number of soot nuclei, leading to higher particle number concentration. With increasing engine load, particle number-size distribution shifted toward bigger ($D_p \sim$ 100 nm) particle sizes. These results were similar to the findings of other researchers.[29,37−40] An increasing EGR rate led to higher particle number concentration (Figures 10a-c). At 0% EGR rate, particle number concentration increased with increasing T_i. At 10 and 20% EGR rates, particle number concentration varied depending on the dominance of T_i and EGR. This trade-off was due to two opposite effects caused by an increasing EGR rate and increasing T_i. An increasing EGR rate reduced peak in-cylinder temperature and enhanced the tendency of particle agglomeration; however, increasing T_i resulted in higher soot nucleation. At all loads and EGR rates, increasing T_i shifted the particle number-size distribution curve toward smaller particle sizes. This showed that increasing T_i produced a higher number of particulates. Relatively lesser
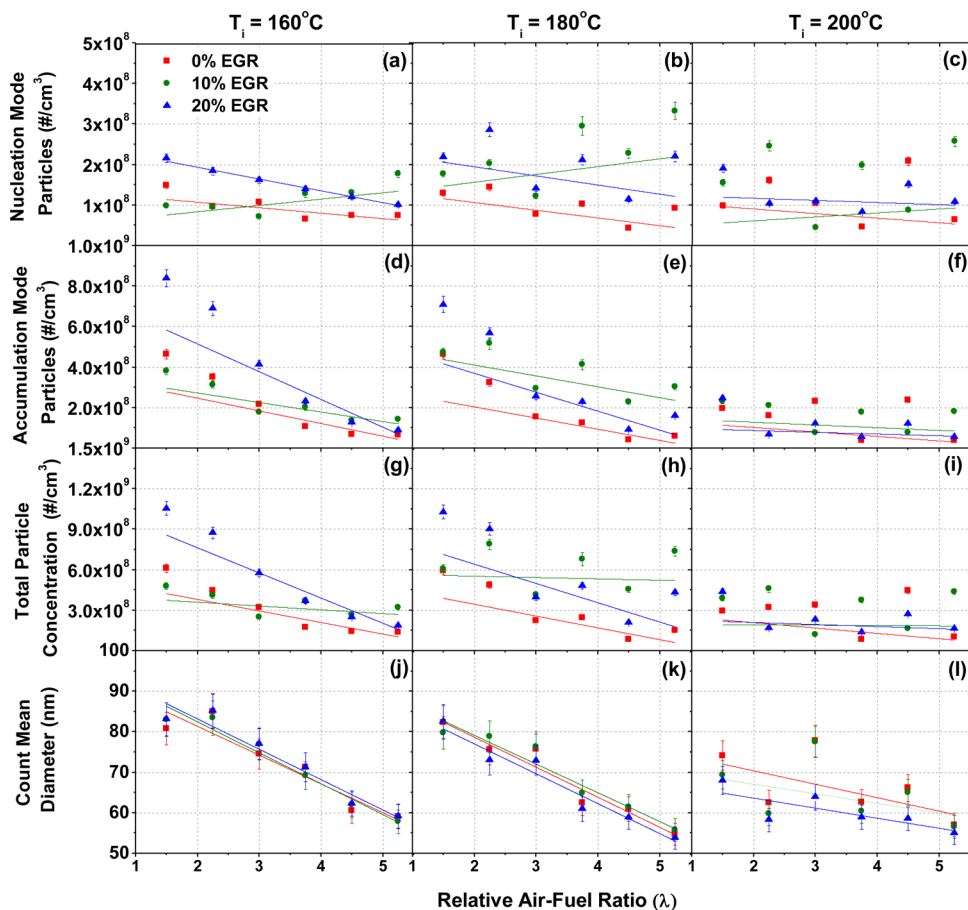
Figure 13. NMP, AMP, and TPN concentrations and CMD of particulates emitted by mineral diesel fueled PHCCI engine at different loads, T_i's, and EGR rates.

soot agglomeration at higher T_i was the main reason for this trend, which resulted in slightly higher particulates of smaller size. At higher T_i, pyrolysis of lubricating oil also contributed to particulate formation although the contribution of lubricating oil to particulate formation might be limited. With increasing T_i, breakdown of lubricating oil film present on the cylinder walls led to formation of different PAHs, which acted as a soot precursor and increased particulate numbers.[35,42] Overall, based on particle number-size distribution, it can be stated that 10% EGR rate was effective at higher engine loads, while 20% EGR rate showed improved particulate characteristics at lower engine loads (Figures 10o and r). Among all experimental conditions, maximum particle number concentration was ~4 × 10^8 particles/cm^3 of exhaust gas at λ = 1.5, 30% EGR, and T_i = 160 °C.

Particle surface area-size distribution showed the presence of toxic species on particulate surface. Higher surface area provides more sites for condensation of harmful gaseous species and PAHs, which in turn increased toxicity of these particulates. For surface area calculations, particulates were assumed to be spherical, and surface area was calculated by using the following equation:[42,43]

$$dS = dN \cdot (D_p)^2$$

Here dS is the surface area of the particles in the given size range having mean diameter D_p, and dN is the number concentration of particulate with mean diameter D_p. For the same particulate mass, smaller particulates offer higher surface area compared to larger particles. Therefore, smaller particulates are more hazardous to human health compared to larger particles.[44,45]

Figures 11a-r show particle surface area-size distribution at different engine loads, T_i's, and EGR rates. It is observed that particle surface area increased with increasing engine load (Figures 11a, d, g, j, m, and p). Employing EGR resulted in slightly higher particle surface area due to condensation of less volatile species at relatively lower in-cylinder temperatures. Increasing T_i led to lower particle surface area at higher engine loads (λ = 1.5 and 2.25, Figures 11a-f); however, at lower engine loads (λ = 3.0 to 5.25, Figures 11g-r), particulate surface area distribution slightly increased with increasing T_i. Particle surface area-size distribution showed that particle size corresponding to maximum particle surface area ranged from 80 to 120 nm with maximum particle surface area being ~8 × 10^{12} nm^2/cm^3 of exhaust gas.

Figures 12a-r showed particulate mass-size distribution of mineral diesel fueled PHCCI engine at different engine loads, T_i's, and EGR rates. Particle mass was calculated from particle size-number distribution, assuming constant particulate density (1.0 g/cm^3).[42,43] Higher particle mass-size distribution increased the possibility of particles settling down to the ground rather quickly. Lighter particles are more harmful compared to heavier particles since they have higher ambient retention times and remain suspended in the ambient air for longer periods of time. This increases the possibility of them being inhaled by humans thus leading to harmful health issues.

Figure 12 also showed that particulate mass increased with increasing engine load due to the presence of higher fuel quantity in the combustion chamber, which promoted particulate formation. The mass-size distribution curve shifted upward-right with increasing engine load (Figures 12a, d, g, and j), which showed the dominance of larger particles in the particulate mass distribution. It can be seen that nanoparticles showed significant contribution to particle number concentration (Figure 10); however, their contribution to particle mass was almost insignificant. At higher engine loads, particle mass decreased with increasing T_i, but at lower engine loads, particle mass increased with increasing T_i. Variations in the EGR rate also showed an irregular pattern of particulate mass at higher engine loads. However, variation in particulate mass at a different EGR rate was insignificant. Maximum variation in particulate mass was observed at $T_i = 180$ °C (Figures 12b, e, h, k, n, and q), and maximum particulate mass was $\sim 10^5$ μg/m^3 of the exhaust gas.

Figure 13 showed the variations in NMP ($D_p < 50$ nm) (Figures 13a-c), AMP (50 nm $< D_p < 1000$ nm) (Figures 13d-f), total particle number (TPN) (Figures 13g-i) concentrations, and count mean diameter (CMD) (Figures 13j-l) of particulates emitted at different engine loads, EGR rates, and T_i's in PHCCI combustion mode.

Results showed that increasing engine load resulted in higher NMP at 0 and 20% EGR rates; however, 10% EGR rate showed slightly lower NMP at higher engine load (Figures 13a-c). These results were in agreement with the results of particle number-size distribution (Figure 10). The variation in NMP at different operating conditions was not significant. The difference in particle number concentration was attributed mainly to AMP. AMP increased with increasing engine load (Figures 13d-f). At higher engine load, the presence of higher fuel quantity in the combustion chamber and intense in-cylinder conditions were the main reasons for this trend. An increasing EGR rate showed random behavior at different T_i's. At lower T_i, maximum AMP was observed at 20% EGR rate, which decreased with increasing T_i (Figures 13d-f). At higher T_i ($T_i = 180$ and 200 °C), 10% EGR rate resulted in the highest number of AMP. Due to higher AMP at higher engine loads, TPN increased with increasing engine load. TPN varied with the EGR rate, depending upon T_i.

TPN slightly decreased with increasing T_i (Figures 13g-i). The average size of particles emitted by the engine can be represented by CMD, which provides a basis for comparing the overall average size of the particulate emitted at different engine operating conditions. CMD increased with increasing engine load. This was attributed to emission of a large number of larger particles at higher engine loads. Increasing T_i resulted in slightly lower CMD (Figures 13j-l) of the particulate. Lower condensation of volatile species at higher T_i prevented formation of larger particles, which resulted in smaller CMD. At lower T_i ($T_i = 160$ °C), CMD increased with an increasing EGR rate; however, at higher T_i's, high EGR resulted in relatively lower CMD (Figure 13j).

4. CONCLUSIONS

Lower volatility of mineral diesel is one of the main challenges in achieving LTC, which results in inferior fuel-air mixing. This study explored the possibility of mineral diesel fueled LTC by employing an external fuel-air mixture preparation technique using a fuel vaporizer. For a better understanding of PHCCI combustion, experiments were performed at different engine

loads, T_i's, and EGR rates. Results showed that PHCCI combustion was stable at medium engine loads. At higher engine loads, severe knocking led to excessive noise and increased NOx emissions. EGR emerged as an effective tool to control combustion phasing and HRR, especially at higher engine loads. Application of EGR shifted combustion phasing into optimum range and improved both combustion and performance compared to no EGR condition. With increasing the EGR rate, NOx emissions significantly reduced; however, at 20% EGR rate, in-cylinder fuel-air mixture dilution led to retarded combustion phasing and degraded engine performance due to higher HC and CO emissions. At higher EGR rates, combustion stability deteriorated and resulted in slightly higher particulate emissions. This was improved by increasing T_i, which affected fuel-air mixing, leading to slightly lower CO and HC emissions at 180 °C. Increasing T_i improved the combustion stability at low loads; however, higher T_i led to the thermal throttling effect, which reduced the oxygen concentration (increased λ) in the fuel-air mixture, resulting in unstable combustion (excessive knocking at 200 °C) at intermediate loads. At higher engine loads, increasing T_i led to excessive knocking. Therefore, it can be concluded that intermediate EGR ($\sim$10%) and T_i ($\sim$180 °C) were suitable for PHCCI combustion mode.

Overall, this study demonstrated experimentally that the fuel vaporizer improved fuel-air mixing, leading to superior PHCCI combustion. At extreme engine loads (knocking and misfire limits), PHCCI combustion can be effectively controlled by a combination of suitable control parameters namely T_i and EGR, thereby extending the operating window of this combustion mode.

■ AUTHOR INFORMATION

Corresponding Author
*E-mail: akag@iik.ac.in.
ORCID
Avinash Kumar Agarwal: 0000-0002-7777-785X
Notes
The authors declare no competing financial interest.

■ LIST OF ABBREVIATIONS

aBDC = after top dead center
AMP = accumulation mode particles
aTDC = after top dead center
bBDC = before top dead center
BSOF = benzene soluble organic fraction
bTDC = before top dead center
CI = compression ignition
CIHC = compression ignition homogeneous charge
CO = carbon monoxide
COV = coefficient of variation

DI = direct injection
DPF = diesel particulate filter
EGR = exhaust gas recirculation
EGT = exhaust gas temperature
EoC = end of combustion
HC = hydrocarbons
HRR = heat release rate
ISFC = indicated specific fuel consumption
ITE = indicated thermal efficiency
KI = knock integral
KP = knock peak
LNT = lean NOx trap
LTC = low temperature combustion
MFB = mass fraction burned
NA = naturally aspirated
NMP = nucleation mode particles
NOx = oxides of nitrogen
PAHs = polycyclic aromatic hydrocarbons
PFI = port fuel injection
PHCCI = partially premixed homogeneous charge compression ignition
PM = particulate matter
R_{max} = maximum rate of pressure rise
SCR = selective catalytic reduction
SI = spark ignition
SoC = start of combustion
T_i = intake charge temperature
TTL = transistor-transistor logic

■ REFERENCES

(1) Akihama, K.; Takatori, Y.; Inagaki, K.; Sasaki, S.; Dean, A. M. Mechanism of the smokeless rich diesel combustion by reducing temperature. SAE Technical Paper 2001-01-0655; 2001.

(2) Environmental Protection Agency, USA. http://www.epa.gov/acidrain/what/ (accessed September 2011).

(3) Maricq, M. M. Chemical characterization of particulate emissions from diesel engines: A review. J. Aerosol Sci. 2007, 38, 1079−1118.

(4) Onishi, S.; Jo, S. H.; Shoda, K.; Jo, P.; Kato, S. Active thermo-atmosphere combustion (ATAC)-a new combustion process for internal combustion engines. SAE Technical Paper 790501; 1979.

(5) Najt, P. M.; Foster, D. E. Compression-ignited homogeneous charge combustion. SAE Technical paper 830264; 1983.

(6) Thring, R. H. Homogeneous-charge compression-ignition (HCCI) engines. SAE Technical paper 892068; 1989.

(7) Stockinger, V.; Schapertons, H.; Kuhlmann, U. Investigations on a gasoline engine working with self-ignition by compression. MTZ. Vole. 1992, 53, 80−5.

(8) Olsson, J.-O.; Tunestål, P.; Johansson, B. Closed-loop control of an HCCI engine. SAE Technical Paper 2001-01-1031; 2001.

(9) Takeda, Y.; Keiichi, N.; Keiichi, N. Emission characteristics of premixed lean diesel combustion with extremely early staged fuel injection. SAE Technical Paper 961163; 1996.

(10) Iwabuchi, Y.; Kawai, K.; Shoji, T.; Takeda, Y. Trial of new concept diesel combustion system − Premixed compression-ignited combustion. SAE Technical Paper 1999-01-0185; 1999.

(11) Nordgren, H.; Hultqvist, A.; Johansson, B. Start of Injection Strategies for HCCI combustion. SAE Technical Paper 2004-01-2990; 2004.

(12) Harada, A.; Shimazaki, N.; Sasaki, S.; Miyamoto, T.; Akagawa, H.; Tsujimura, K. The effects of mixture formation on premixed lean diesel combustion. SAE Technical Paper 980533; 1998.

(13) Ishima, T.; Matsuda, T.; Shiga, S.; Araki, M.; Nakamura, H.; Obakata, T.; Yang, X.; Long, W.-Q.; Murakami, A. Characteristics of HCCI Diesel Combustion Operated with a Hollow Cone Spray. SAE Technical Paper 2003-01-1823; 2003.

(14) Miles, P. C.; Choi, D.; Pickett, L. M.; Singh, I. P.; Henein, N.; Rempel Ewert, B. A.; Yun, H.; Reitz, R. D. Rate-Limiting Processes in Late-Injection, Low-Temperature Diesel Combustion Regimes. THIESEL International Conference on Thermo and Fluid Dynamic Processes in Diesel Engines; 2004.

(15) Wimmer, A.; Eichlseder, H.; Klell, M.; Figer, G. Potential of HCCI concepts for DI diesel engines. International Journal of Vehicle Design 2006, 41 (1−4), 32−48.

(16) Stanglmaier, R. H.; Roberts, C. E. Homogeneous charge compression ignition (HCCI): benefits, compromises, and future engine applications. SAE Technical Paper 1999-01-3682; 1999.

(17) Gray, A. W.; Ryan, T. W., III Homogeneous charge compression ignition of diesel fuel. SAE Technical Paper 971676; 1997.

(18) Ryan, T. W.; Callahan, T. J. Homogeneous charge compression ignition of diesel fuel. SAE Technical Paper 961160; 1996.

(19) Baumgarten, C. Mixture formation in internal combustion engines; Springer Science & Business Media: 2006.

(20) Suzuki, H.; Koike, N.; Ishii, H.; Odaka, M. Exhaust purification of diesel engines by homogeneous charge with compression ignition part 1: Experimental investigation of combustion and exhaust emission behavior under pre-mixed homogeneous charge compression ignition method. SAE Technical Paper 970313; 1997.

(21) Christensen, M.; Hultqvist, A.; Johansson, B. Demonstrating the multi fuel capability of a homogeneous charge compression ignition engine with variable compression ratio. SAE Technical Paper 1999-01-3679; 1999.

(22) Canova, M.; Midlam-Mohler, S.; Guezennec, Y.; Rizzoni, G. Theoretical and experimental investigation on diesel HCCI combustion with external mixture formation. International journal of vehicle design. 2007, 44, 62−83.

(23) Midlam-Mohler, S.; Haas, S.; Guezennec, Y.; Bargende, M., Rizzoni, G, Berner, H. J. Mixed mode diesel HCCI-DI with external mixture preparation. FISITA2004 World Automotive Congress, Barcelona, Spain, 23−27 May 2004.

(24) Ganesh, D.; Nagarajan, G. Homogeneous charge compression ignition (HCCI) combustion of diesel fuel with external mixture formation. Energy 2010, 35, 148−157.

(25) Chiara, F.; Canova, M. Mixed-mode homogeneous charge compression ignition—direct injection combustion on common rail diesel engines: An experimental characterization. Int. J. Engine Res. 2009, 10, 81−96.

(26) Puschmann, H.; Buchwald, R.; Pannwitz, M.; Sommer, A.; vom Schloß, H. P.; Lucka, K. Homogeneous diesel combustion with external mixture formation by a cool Flame Vaporizer. SAE Technical Paper 2006-01-3323; 2006.

(27) Canova, M.; Midlam-Mohler, S.; Guezennec, Y.; Rizzoni, G. Mean value modeling and analysis of HCCI diesel engines with external mixture formation. J. Dyn. Syst., Meas., Control 2009, 131, 011002.

(28) Singh, A. P.; Agarwal, A. K. Combustion characteristics of diesel HCCI engine: an experimental investigation using external mixture formation technique. Appl. Energy 2012, 99, 116−25.

(29) Maurya, R. K.; Agarwal, A. K. Experimental investigation of the effect of the intake air temperature and mixture quality on the combustion of a methanol-and gasoline-fuelled homogeneous charge compression ignition engine. Proc. Inst. Mech. Eng., Part D 2009, 223, 1445−58.

(30) Atkins, M.; Koch, C. The effect of fuel octane and diluent on homogeneous charge compression ignition combustion. Proc. Inst. Mech. Eng., Part D 2005, 219, 665−675.

(31) Yao, M.; Zhang, B.; Zheng, Z.; Chen, Z.; Xing, Y. Effects of exhaust gas recirculation on combustion and emissions of a homogeneous charge compression ignition engine fuelled with primary reference fuels. Proc. Inst. Mech. Eng., Part D 2007, 221, 197−213.

(32) Yang, J. Expanding the operating range of homogeneous charge compression ignition-spark ignition dual-mode engines in the homogeneous charge compression ignition mode. Int. J. Engine Res. 2005, 6, 279−88.

(33) Agarwal, A. K.; Singh, A. P.; Lukose, J.; Gupta, T. Characterization of exhaust particulates from diesel fueled homogenous charge compression ignition combustion engine. *J. Aerosol Sci.* **2013**, *58*, 71−85.

(34) Asad, U.; Zheng, M.; Ting, DS-K; Tjong, J. Implementation challenges and solutions for homogeneous charge compression ignition combustion in diesel engines. *J. Eng. Gas Turbines Power* **2015**, *137*, 101505.

(35) Singh, A. P.; Agarwal, A. K. Diesoline, diesohol and diesosene fuelled HCCI engine development. *J. Energy Resour. Technol.* **2016**, *138*, 052212.

(36) Singh, A. P.; Agarwal, A. K. Effect of intake charge temperature and EGR on biodiesel fuelled HCCI engine. SAE Technical Paper 2016-28-0257; 2016.

(37) Franklin, L. *Effects of homogeneous charge compression ignition (HCCI) control strategies on particulate emissions of ethanol fuel*; University of Minnesota, 2010.

(38) Kittelson, D. B. Engines and nano-particles: a review. *J. Aerosol Sci.* **1998**, *29* (5−6), 575−88.

(39) Agarwal, A. K.; Gupta, T.; Lukose, J.; Singh, A. P. Particulate characterization and size distribution in the exhaust of a gasoline homogeneous charge compression ignition engine. *Aerosol Air Qual. Res.* **2015**, *15*, 504−16.

(40) Aceves, S. M.; Flowers, D. L. A detailed chemical kinetic analysis of low temperature non-sooting diesel combustion. SAE Technical Paper 2005-01-0923; 2005.

(41) User Manual of AVL Indo-micro software. *Exploration Guide: AVL INDICOM 2014*; AVL List GmbH: Graz, Austria, 2014.

(42) Singh, A. P.; Pal, A.; Agarwal, A. K. Comparative particulate characteristics of hydrogen, CNG, HCNG, gasoline and diesel fueled engines. *Fuel* **2016**, *185*, 491−9.

(43) *Engine Exhaust Particle Sizer spectrometer model 3090*; Operation and service manual. TSI: USA; March 2009.

(44) Agarwal, A. K.; Dhar, A.; Srivastava, D. K.; Maurya, R. K.; Singh, A. P. Effect of fuel injection pressure on diesel particulate size and number distribution in a CRDI single cylinder research engine. *Fuel* **2013**, *107*, 84−89.

(45) Schlesinger, R. B.; Kunzli, N.; Hidy, G. M.; Gotschi, T.; Jerrett, M. The health relevance of ambient particulate matter characteristics: coherence of toxicological and epidemiological inferences. *Inhalation Toxicol.* **2006**, *18*, 95−125.